JOURNAL OF CATALYSIS **146**, 346–357 (1994)

Transient Studies on Reaction Steps in the Oxidative Coupling of Methane over Catalytic Surfaces of MgO and Sm_2O_3

O. V. Buyevskaya,[1] M. Rothaemel, H. W. Zanthoff, and M. Baerns[2]

Lehrstuhl für Technische Chemie, Ruhr-Universität Bochum, D-44780 Bochum, Germany

Received March 22, 1993; revised September 9, 1993

Adsorption of CH_4 and O_2 as well as surface reactions of CH_4, CD_4, and CH_4–CD_4 mixtures in the absence and presence of gas-phase oxygen were studied over MgO and Sm_2O_3 in the temperature range from 373 to 1073 K applying the temporal analysis of products (TAP) reactor. Formation of $CH_3\cdot$ radicals was observed during surface reaction of methane in the Knudsen-diffusion regime while ethane and ethylene were detected only at increasing pulse intensity, i.e., in the molecular-diffusion regime. The reactivity of surface-lattice oxygen of MgO and Sm_2O_3 was studied in the Knudsen regime with respect to the H–D exchange in methane. Surface hydroxyl groups were found to participate in this reaction, but no direct interaction of methane molecules on the catalyst surface occurred. H–D exchange proceeds via a multistep mechanism involving methane-surface interaction leading to dissociative adsorption of methane. The pathways of surface-oxygen species of short lifetimes were monitored using sequential pulses of oxygen and methane having various time intervals between 0.02 and 20 s. On MgO, surface-lattice oxygen is responsible for methyl radical formation resulting in C_2 hydrocarbons, while adsorbed oxygen species have very short lifetimes (<0.1 s) on the surface and take part in the reactions of total oxidation. On Sm_2O_3, active oxygen species formed by the interaction of gaseous O_2 with the catalyst surface have lifetimes up to 20 s and are mainly responsible for methane conversion and product formation. Based on the response analysis it was assumed that direct interaction of gas-phase methane with active oxygen surface species is the first step in the oxidative coupling of methane (OCM) over Sm_2O_3. It was found that the type of methane activation which takes place in H–D exchange was not involved in the OCM reaction over Sm_2O_3. The interaction of C_2H_6, CO, and CO_2 with the surface of Sm_2O_3 was also studied. C_2H_6 was converted to C_2H_4 and CO_x; CO was effectively oxidized to CO_2, which was strongly adsorbed on Sm_2O_3 up to T = 1073 K. © 1994 Academic Press, Inc.

INTRODUCTION

The surface processes in the catalyic oxidative coupling of methane (OCM) to ethane and by subsequent dehydrogenation to ethylene, especially the nature of methane activation and the role of lattice versus adsorbed oxygen in the product formation are not yet fully understood. C–H bond breaking is widely believed to be involved in the initial rate-controlling reaction step in C_2 formation since kinetic isotope effects (k_H/k_D) have been observed over several different catalysts (1–7). However, the details of methyl-radical formation and the nature of active sites are still subjects of discussion. Two general points of view exist regarding the first step of methane interaction with the catalyst surface. According to Refs. (8–11), methyl radicals are formed directly in the reaction of gas-phase methane with active oxygen surface species in an Eley–Rideal-type mechanism. On the other hand, dissociative adsorption of methane was suggested to proceed during the OCM reaction (5, 12–16). The isotopic exchange of CH_4–CD_4 and CH_4–D_2 was used by several authors to study methane activation in the OCM reaction (3, 5, 13, 14, 16). Results of Robertson *et al.* for Al_2O_3 at 284–360 K (17), for MgO at 623–683 K (18), and of Bird *et al.* for La_2O_3 at 625 K (19), and of Utajama *et al.* for alkaline earth metal oxides and La_2O_3 at 573 K (20) showed that H–D exchange in methane involves heterolytic dissociation of an adsorbed methane molecule on the solid surface.

The understanding of the nature of the active sites on the catalyst surface (lattice vs adsorbed oxygen) and the roles of these sites in the OCM reaction is a subject of great interest. In particular, to estimate the involvement of lattice oxygen in the product formation some authors have used a comparison of reaction rates in the presence and absence of oxygen in the reaction mixture (21–23). More recently some transient techniques such as steady-state isotopic transient kinetic analysis (24), experiments using the TAP reactor (25), temperature programmed isotopic exchange between gas-phase and lattice oxygen (26), and step changes in $^{16}O_2$ and $^{18}O_2$ feeds (27) were applied to elucidate the role of oxygen in the OCM reaction. However, this problem has not yet been fully clarified.

In the present work, results are reported for adsorption of CH_4 and O_2 as well as for surface reactions of CH_4,

---

[1] Boreskov Institute of Catalysis, Novosibirsk, 630090, Russia.

[2] To whom correspondence should be addressed. email: baerns@risc.techem.ruhr-uni-bochum.de

021-9517/94 $6.00

CD_4, and a CH_4–CD_4 mixture over two different catalysts, i.e., MgO and Sm_2O_3 applying a transient pulse technique by using the temporal analysis of products (TAP) reactor. For experiments with pulse sizes of 10^{15} molecules, the gas flow through the reactor proceeds only by Knudsen diffusion, i.e., without gas-phase collisions. This made it possible to study solely the heterogeneous steps during the oxidative coupling of methane, such as methane and oxygen adsorption, methyl radical formation, methane activation, and the surface interaction of products (C_2H_6, CO, CO_2). To investigate the factors responsible for ethane formation, experiments were performed also with methane pulses of higher intensity resulting in gas transport by molecular diffusion.

Using the advantages of the TAP reactor the mechanism of methane activation during H–D exchange on MgO and Sm_2O_3 surfaces was studied in the temperature range corresponding to the OCM reaction (923–1073 K). Furthermore, the participation of hydroxyl groups which are known to exist on the surfaces of MgO (28) and Sm_2O_3 (29) even after evacuation at high temperatures, was examined. Also investigated was how the methane activation which proceeds during H–D exchange is related to the OCM reaction.

Furthermore, the pathways and lifetimes of active oxygen species formed by the interaction of gas-phase O_2 with the catalyst surfaces was monitored directly and the activity of these sites compared to lattice oxygen was estimated. The role of adsorbed oxygen in methane conversion and product formation was studied using sequential pulses of oxygen and methane with various time intervals (0.02–20 s).

From the results of the experiments described an advanced understanding of the elementary processes in the OCM reaction was expected.

METHODS

Catalyst Preparation and Characterization

The catalytic materials applied in the present work were prepared as follows: MgO (S_{BET} = 9.8 m^2/g): calcination of $Mg(NO_3)_2 \cdot 6\,H_2O$ at 1073 K for 3 h. Sm_2O_3 (S_{BET} = 2.3 m^2/g): calcination of $Sm(NO_3)_3 \cdot 6\,H_2O$ at 1123 K for 3 h. After calcination the materials were pelletized and crushed, and the 255–350 μm fraction was separated for catalytic and adsorption experiments. The phase composition of Sm_2O_3 which existed only in its cubic form was determined by XRD. The specific surface areas were measured by the 1-point BET method using N_2 adsorption at 77 K.

TAP reactor

The TAP reactor system applying a transient pulse technique in vacuum with high time resolution has been described elsewhere in detail (30). Therefore, only a brief overview of the operating principle and the specific conditions for the present work are mentioned below.

Principle. An essential part of the TAP reactor (cf. Fig. 1) consists of two high-speed beam valves (Newport Company) which can produce pulses of a half-width of less than 10 μs (30) containing approx. 10^{14}–10^{18} molecules per pulse. The gas pulse (inlet signal) enters the microcatalytic fixed-bed reactor which is located in high vacuum (approx. 10^{-4} Pa). The response signal at the reactor outlet is the temporal change of the intensity of the compounds leaving the TAP reactor which is analyzed by a UTI 100 C quadrupole mass spectrometer with high time resolution (up to 10 μs). The response strongly depends on the interaction of the compounds with the catalytic materials (adsorption, desorption, reaction). The signal is afterwards analyzed with respect to its zeroth and first moment; the zeroth moment corresponds to the total detected amount of the compound and the first moment to its mean residence time. Due to the high time resolution even weak adsorption/desorption processes can be monitored; furthermore, short-lived reaction intermediates desorbing from the surface can be detected.

Operating conditions. Pulse sizes of approx. 10^{15} and 10^{17} molecules were used to obtain pulses corresponding to the pressure regime of Knudsen diffusion, i.e., without any gas-phase collisions, and to the intermediate regime between Knudsen and molecular diffusion, i.e., with a significant amount of gas-phase collisions. For simplification, the experiments with pulses of approx. 10^{17} molecules per pulse are referred to as the "molecular diffusion regime". The mainfold was kept at a constant temperature of 333 K to improve pulse stability. Nevertheless, the pulse size decreased by about 30% when heating the reactor from 303 to 1073 K. Hence, all gas mixtures contained 5 or 10% of an inert gas (Ar, Ne, or He) as an internal standard to control the reproducibility of the pulses and to allow the calculation of conversions and the respective selectivities.

The microcatalytic fixed-bed reactor made of Inconel had an inner diameter of 5.4 mm and a total bed length of 28 mm. A temperature gradient over the whole reactor length was determined in separate experiments under steady-state in vacuum; inside the catalyst bed the maximal axial gradient amounted to 10 K. For each experiment 690 mg of catalyst (fraction 250–355 μm) was packed between two layers of quartz of the same particle size; the catalyst volume amounted to about one-third of the total bed volume. Before each experiment the catalyst was pretreated with O_2 pulses at 1073 K until a stable oxygen response was observed. Then the reactor was kept evacuated at approx. 10^{-4} Pa for 10 min before the

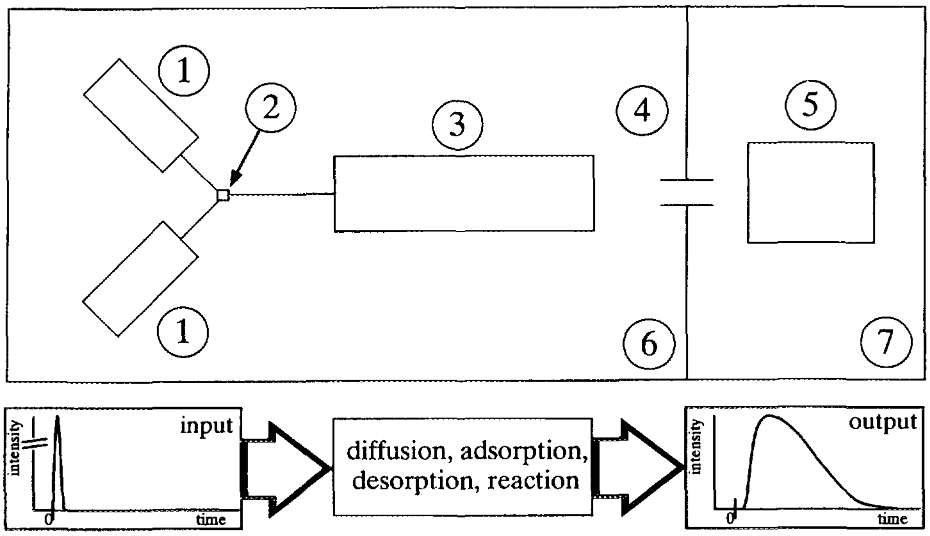

FIG. 1. Scheme of the Temporal analysis of products (TAP) reactor. (1) High-speed pulse valves, (2) zero-volume manifold, (3) fixed-bed reactor, (4) focussing slits, (5) quadrupole mass spectrometer, (6) reaction chamber ($P \approx 10^{-4}$ Pa), and (7) detection chamber ($P \approx 10^{-7}$ Pa).

reaction mixture was pulsed over the catalyst surface. To reduce the signal-to-noise ratio in the response, the responses of six to ten pulses were averaged; this procedure is justified since due to the small amounts pulsed only an insignificant proportion of the catalyst (<1%) is covered by adsorbed and/or reacting species. The mean residence times of the gas molecules in the reactor amounted to 60–200 ms except for CO_2 where the residence times were much higher.

For the various experiments the following reaction mixtures were used: CH_4-CD_4-Ar = 10 : 10 : 1, $CH_4(CD_4)$-(Ar, Ne) = 1 : 1, C_2H_6-Ne = 1 : 1, CO-He = 1 : 10, and CO_2-He = 1 : 19. Simultaneous pulses of the above-mentioned mixtures and oxygen from the two beam valves were used to obtain mixtures containing O_2. The influence of adsorbed oxygen species on the surface reaction of methane was studied in transient experiments with sequential pulses of oxygen and the reactant. First, the oxygen pulse was introduced, then a methane pulse was supplied to the reactor after different time intervals (0.02–20 s). For each experiment this procedure was repeated six to ten times with a constant time interval between methane and oxygen pulses (1 s), and then the averaged responses were used. TPD experiments were carried out with a linear heating rate of 25 K/min in high vacuum at a total pressure of approx. 10^{-4} Pa.

Chemicals

$Mg(NO_3)_2 \cdot 6H_2O$ (purity: 99.9%, Baker Chemicals) and $Sm(NO_3)_3 \cdot 6\ H_2O$ (purity: 99.9%, Aldrich) were applied for catalyst preparation.

High purity CH_4 (99.95%), C_2H_6 (99.95%), O_2 (99.996%), H_2 (99.999%), CO (99.998%), CO_2 (99.995%), Ar (99.995%), Ne (99.998%), and He (99.999%) from Messer–Griesheim (Oberhausen, Germany) and CD_4 (isotopic purity 99.9 at % D) from MSD Isotopes (Ismaning, Germany) were used in the experiment.

Quantitative Data Evaluation

The following atomic masses (amu) were used for the identification of the different compounds: 44 (CO_2); 40 (Ar); 32 (O_2); 30, 29 (C_2H_6); 28 (CO_2, CO, C_2H_6, C_2H_4); 26, 25 (C_2H_6, C_2H_4); 20 (CD_4); 19 (CD_3H); 18 (CD_4, CD_3H, CD_2H_2); 17 (CD_3H, CD_2H_2, CDH_3); 16 (CH_4); 15 ($CH_3\cdot$, CH_4); 4 (He). The fragmentation patterns of all substances were experimentally determined in order to calculate the contributions of different compounds to a measured amu signal. Only for isotopic methanes (amu = 17 to 19) were data for fragmentation patterns taken from the literature (31). To calculate yields and selectivities the relative sensitivities of CH_4, C_2H_6, C_2H_4, CO, CO_2, and O_2 were determined according to their different ionization probabilities. The sensitivities were calculated with respect to the sum of all fragment peaks in the mass spectrum of the different compounds instead of using the most intense peak as the basis. The sensitivities of isotopic methanes were assumed to be similar to CH_4 according to Ref. (31).

Several methods have been described for the detection of methyl radicals in the OCM reaction (8, 10, 32, 33). In the present work, the amount of methyl radicals formed was calculated from the ratio of amu 15 to amu 16 corrected by the CH_4 fragmentation pattern. For this calculation it was assumed that the sensitivity of detection of CH_4 and methyl radicals in the quadrupole mass spectrometer is equal. Thus, the reported values for yield and selectivity of $CH_3\cdot$ formation should be considered as having arbitrary units although the observed patterns are certainly valid.

Determination of the Interaction of Gases with Catalyst Surfaces

When passing gas through the reactor without any interaction with the surface, the first moment of the response signal at the reactor outlet, i.e., the mean residence time t_i of a compound i, is proportional to its molar mass M_i according to diffusion theory. Hence, if the ratio of the residence times of a probe molecule t_p and of an inert gas t_{inert} is higher than the ratio of the square roots of the corresponding molar masses, the probe molecule interacts reversibly with the catalyst surface:

$$t_p/t_{inert} > (M_p/M_{inert})^{1/2}.$$

This relationship is only valid in the absence of the consumption of reactant i, because any reaction would influence the resulting response curve.

Adsorption enthalpies were derived from the temperature dependence of the first moment of the response compared to the inlet signal. This procedure was based on the solution of the differential mass balance describing the transient behaviour of the reactor (see Gleaves *et al.* (30)).

RESULTS

I. Interaction of CH_4, C_2H_6, CO_2, CO, and O_2 with the Catalyst Surfaces

The surface interaction of various compounds involved in the OCM reaction was investigated on Sm_2O_3 (CH_4, C_2H_6, CO_2, CO, O_2) and on MgO (CH_4, O_2). The experiments were performed in the pressure regime of Knudsen diffusion, i.e., in the absence of gas-phase collisions, and hence any gas-phase reactions. Hereby, the study of the heterogeneous activation steps and surface reaction pathways of these molecules was made possible.

(*a*) Sm_2O_3

CH_4. Transient experiments with CH_4 pulses in the Knudsen regime were performed in the temperature range from 373 to 1035 K. The results of the moment analysis showed a weak adsorption of methane at low temperatures (<723 K) with an adsorption enthalpy of ca. −5 ± 2 kJ/mol (cf. Fig. 2), and no methane conversion occurred. At temperatures higher than 723 K no adsorption of methane could be determined by the moment analysis. At temperatures above 723 K conversion of methane occurred, and increased from 3% at 723 K to 19% at 1035 K. Methyl radicals and CO were observed at the reactor outlet; the activation energy E_a of the overall process amounted to ca. 70 kJ/mol, as derived from the temperature dependence of CH_4 conversion. No ethane and ethylene, however, was observed. CO_2, which might be formed during the reaction, was also not detected, possibly due to its absorption on the catalyst surface (CO_2 interaction, see below).

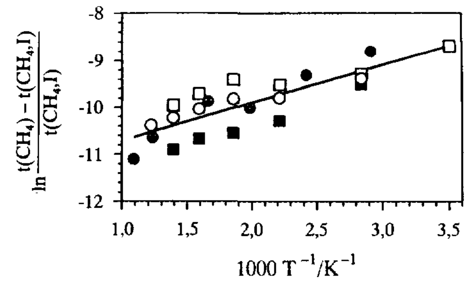

FIG. 2. Temperature dependence of the mean residence time of CH_4 in Knudsen diffusion regime over Sm_2O_3 ($t(CH_4)$ = experimentally observed first moment, $t(CH_4, I)$ = calculated first moment of an inert molecule with amu 16). (●) Run 1, (○), run 2, (■) run 3, and (□) run 4.

The temperature dependence of $CH_3\cdot$ yield and selectivity is shown in Fig. 3. The maximum yield of methyl radicals was observed at 1035 K, while the selectivity for radical formation decreased with increasing temperature. When applying pulse sizes leading to the molecular diffusion regime, i.e., increasing the probability of gas-phase collisions, the formation of radicals decreased and ethane was detected.

C_2H_6. The interaction of ethane in the Knudsen-diffusion regime with the catalyst surface was studied using an equimolar C_2H_6-Ne mixture. Reversible adsorption was detected below 540 K (ΔH = −25 ± 4 kJ/mol); no adsorption was observed at higher temperatures. At 540 K ethane conversion (X) started to occur ($X_{C_2H_6}$ = 4%) and increased up to 83% at 1035 K (cf. Table 1). From the temperature dependence of overall ethane consumption an activation energy of ca. 29 kJ/mol was derived. The main product of the surface reaction was ethylene. Its yield passes through a maximum at 991 K (ca. 56%), while its selectivity decreased steadily with increasing temperature. Simultaneously, CO selectivity and yield increased.

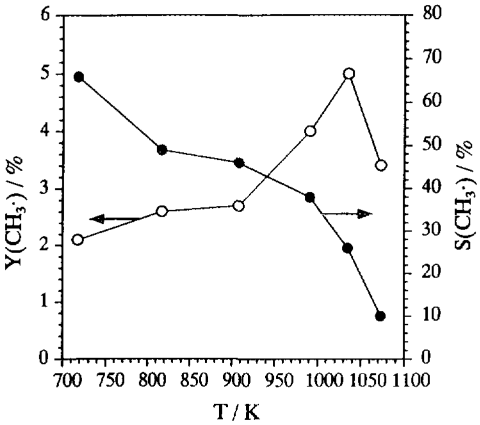

FIG. 3. Dependence of yield (Y) and selectivity (S) of methyl radical formation on temperature during the surface reaction of CH_4 on Sm_2O_3 in the Knudsen-diffusion regime.

TABLE 1

Surface Reaction of Ethane over Sm_2O_3 Studied by Pulse Experiments at Different Temperatures in the Knudsen-Diffusion Regime: Dependence of C_2H_6 Conversion (X), CO and C_2H_4 Selectivity (S), and Yield (Y) on the Temperature

T (K)	$X(C_2H_6)$ (%)	$S(C_2H_4)$ (%)	$Y(C_2H_4)$ (mole%)	$S(CO)$ (%)	$Y(CO)$ (mole%)
538	3.5	100	3.5	0	0
628	7.9	100	7.9	0	0
718	17.9	91	16.3	9	1.6
817	27.2	91	24.7	9	2.5
908	42.8	89	38.3	11	4.5
991	65.4	86	56.4	14	9.5
1035	83.1	52	42.8	15	12.7

At the highest temperature studied (1035 K) the carbon balance did not amount to 100% (cf. Table 1); hence, it was assumed that at this temperature also CO_2 was formed that could not be detected due to adsorption (see below). The nonselective surface oxidation of ethane over Sm_2O_3 increased with increasing temperature similar to methane conversion.

CO_2. As described above, no CO_2 was detected during the reaction of CH_4 and C_2H_6 with the catalyst surface. It might be assumed that CO_2 formed during the reaction is strongly adsorbed on the surface and/or desorbed too slowly to be detected in the applied time scale (up to 20 s). Therefore, the interaction of CO_2 with the catalyst was investigated using pulse experiments with a CO_2–He (1 : 19) mixture. No CO_2 response was detected up to 1073 K; at this temperature a CO_2 response was observed with a very long residence time (>10 s). These results indicate that the surface of samarium oxide possesses strong binding sites for carbon dioxide. This is supported by the result of a CO_2 TPD experiment which was carried out after treatment of the Sm_2O_3 with CO_2 pulses at 373 K in the TAP reactor. The desorption started at 623 K with a maximum at 988 K; however, even at 1073 K total desorption had not been achieved.

CO. The interaction of CO with the catalyst surface was studied in the Knudsen-diffusion regime with pulses of a CO–He (1 : 10) mixture in the temperature range from 330 to 1073 K to evaluate its reactivity towards oxidation to CO_2. No reversible adsorption was detected. At 723 K 11% CO consumption (i.e., less CO than introduced appearing in the output signal) was observed, and it became nearly complete at 1073 K (94%). No products were observed below 1073 K. At this temperature a broad response of CO_2 was detected similar to the response when CO_2 was directly pulsed.

O_2. No reversible adsorption of O_2 on the oxygen-pretreated catalyst (see Methods) was observed below 723 K. Above this temperature interaction with the surface occurred with increasing extent up to 910 K, and then slightly decreased (cf. Fig. 4).

(*b*) *MgO*

CH_4. The interaction of CH_4 with the catalyst surface was investigated similarly as for Sm_2O_3; however, due to the lower density of MgO compared to Sm_2O_3, the amount was decreased to 200 mg to achieve the same volume of the catalyst layer for avoiding temperature gradients in the catalyst bed. However, the total surface areas are comparable for the applied amounts of both catalysts. No adsorption of CH_4 was detected on the basis of the moment analysis of the response signal up to 820 K; at this temperature the surface reaction started ($X_{CH_4} = 2\%$) increasing to 33% at 1035 K, and methyl radicals, CO, and CO_2 were observed. The detected amount of CH_3 radicals was much lower compared to Sm_2O_3. CO_2 was detected at all temperatures, indicating that the surface of MgO does not possess such strong binding sites for CO_2 as Sm_2O_3. Nevertheless, reversible adsorption of CO_2 takes place on MgO as derived from the moment analysis; the mean residence time amounted to 1–2 s at 1035 K.

O_2. No adsorption was detected in the Knudsen regime at temperatures from 350 to 1073 K as derived from the mean residence time of the oxygen responses.

II. H–D Isotopic Exchange in Methane

The reactivity of the surface lattice oxygen of MgO and Sm_2O_3 was studied with respect to H–D exchange of methane in the Knudsen-diffusion regime. First, an equimolar CH_4–CD_4 mixture was pulsed over the catalysts. For both catalysts, the products included CD_3H, CD_2H_2, methyl radicals, and carbon oxides; this is due to simultaneous isotopic exchange and surface oxidation of methane. Formation of CDH_3 was observed only over Sm_2O_3 at 1023 and 1073 K. Neither ethane nor ethylene was observed. No products were observed in the absence

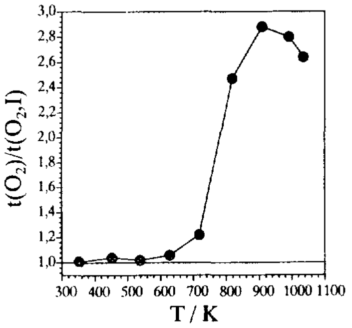

FIG. 4. Interaction of O_2 with the surface of Sm_2O_3 at different temperatures ($t(O_2)$ = experimentally observed mean residence time of the oxygen pulse in the reactor, $t(O_2, I)$ = mean residence time of an inert molecule with the molar mass of 32.

TABLE 2

H–D Isotopic Exchange over MgO and Sm_2O_3 Studied by Pulse Experiments with a CH_4–CD_4 Mixture and CD_4 in the Knudsen-Diffusion Regime: Dependence of the CD_4 Conversion (X) and the Distribution of Isotopic Methanes on Temperature

T(K)	$X(CD_4)$ (%)	Selectivity to exchange (%)	Isotopic distribution after reaction (%)				
			CD_4	CD_3H	CD_2H_2	CDH_3	CH_4
		CH_4–CD_4 mixture over MgO					
923	10	49	47	1	2	0	50
1023	49	20	43	7	1	0	49
1073	81	20	32	14	14	0	42
1073[a]	43	44	39	11	3	0	47
		CH_4–CD_4 mixture over Sm_2O_3					
923	37	78	38	9	7	0	46
1023	72	(80)[b]	18	15	17	5	45
1073	88	(70)[b]	8	10	15	17	51
		Pure CD_4 over Sm_2O_3					
1073	89	49	20	22	25	28	5
1073[a]	75	70	32	34	26	9	0

[a] Reaction after reduction of catalyst surfaces.

[b] Assuming that no CH_4 was formed from CD_4 and that no exchange products were formed from CH_4.

of a catalyst. Results for the CD_4 conversion and selectivity towards H–D exchange and isotopic distribution of products at 923–1073 K are presented in Table 2.

For MgO, reaction at 923 K proceeded mainly to exchange products and methyl radicals. An increase in temperature resulted in rising CD_4 conversion accompanied by a decrease in selectivity towards the formation of H–D exchange products. When the catalyst surface prior to the exchange reaction was reduced by H_2 pulses, CD_4 conversion decreased and selectivity increased with respect to H–D exchange products. Results for product distribution in the reaction of CH_4–CD_4 mixture over MgO showed no formation of CDH_3.

Sm_2O_3 also showed high selectivity in H–D exchange products at 923 K which did not significantly decrease by CO_x formation with increasing temperature. Thus, the activation of methane during the isotopic H–D exchange proceeds with a high selectivity towards exchange products on the oxidized surface of Sm_2O_3 (cf. Table 2). To further study the mechanism of H–D exchange, pulse experiments with pure CD_4 were carried out over Sm_2O_3. Results showed that the H–D exchange proceeds also when pulsing solely CD_4 over the catalyst surfaces. CD_4 conversions in pulse experiments with a CH_4–CD_4 mixture and with pure CD_4 were similar, indicating that the CD_4 interacts only with surface hydrogen. This was supported by results of multipulse experiments with CD_4: it was observed that the formation of exchange products decreased due to the replacement of surface H by D.

The responses of exchange products when pure CD_4 was pulsed over Sm_2O_3 are shown in Fig. 5; it is obvious that the surface reaction of isotopic exchange proceeds stepwise. From Fig. 5 it is also obvious that the exchanged methanes have longer residence times than CD_4, which passes through the reactor without reaction. This indicates a rather strong interaction of methane with the surface during the reaction of H–D isotopic exchange.

III. Transient Studies on the Role of Oxygen in the OCM Reaction

The influence of the presence of gas-phase oxygen on the reaction of methane (CH_4 and CD_4) and the formation of products on Sm_2O_3 and MgO was investigated using simultaneous pulses of CH_4 and O_2 in the molecular-diffusion regime with different methane-to-oxygen ratios. To study the reactivity and lifetime of active oxygen species formed by the interaction of gas-phase oxygen with the catalyst surface, sequential pulses of oxygen followed by methane in various time intervals from 0.02 to 20 s were

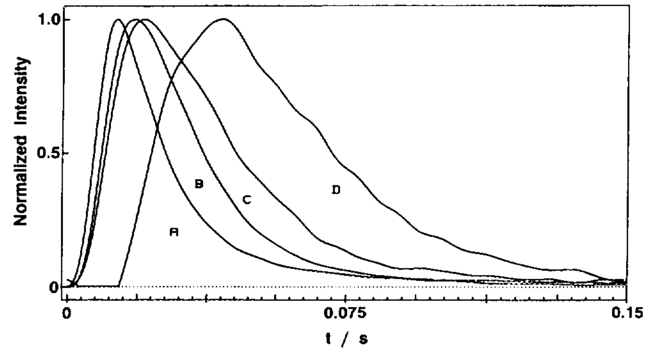

FIG. 5. Normalized transient responses for isotopic methanes formed when pure CD_4 was pulsed over Sm_2O_3 in the Knudsen-diffusion regime at 1073 K (A = CD_4 (enhancement factor k = 1), B = CD_3H (k = 1.05), C = CD_2H_2 (k = 1.36), D = CDH_3 (k = 1.33)).

used. The dependences of methane conversion and product formation on these time intervals were compared for Sm_2O_3 and MgO.

Simultaneous Pulses of Methane and Oxygen

The results for the reaction of CH_4–O_2 mixtures in the molecular-diffusion regime are given in Table 3. In experiments with quartz in the absence of catalyst, formation of CO was observed only for the highest oxygen content in the reaction mixture but no CO_2 and C_2 hydrocarbons were detected.

Sm_2O_3. CH_4 conversion increased significantly with increasing oxygen content in the reaction mixture. A beneficial effect of the presence of gas-phase oxygen on the C_2H_6 formation was observed in the case of a low oxygen content (CH_4–O_2 = 1.5), but increasing the oxygen content resulted in a decrease in selectivity and yield of C_2H_6 (cf. Table 3).

When CD_4 was used an increasing oxygen content resulted in a decrease of the formation of H–D exchange products while C_2D_6 as well as C_2D_5H formation passed through a maximum, as observed for C_2H_6 formation in CH_4–O_2 pulses.

MgO. No remarkable influence of the addition of oxygen to the reaction mixture on the methane conversion was observed. Only at higher oxygen content (CH_4–O_2 = 0.3) did methane conversion increase along with a corresponding decrease in the formation of ethane and CO while a considerable increase in the CO_2 formation was detected. The presence of oxygen in the reaction mixture had no beneficial effect on ethane formation; the amount of ethane formed in the reaction of methane with lattice oxygen was even higher than in the reaction of methane–oxygen mixtures.

TABLE 3

Influence of Oxygen on Methane Conversion and Ethane Formation in the Molecular-Diffusion Regime at 1073 K

		CH_4–O_2		
	CH_4	1.5	0.5	0.3
	Sm_2O_3			
$X(CH_4)$ (%)	14.4	26.5	47.0	72.0
$Y(C_2H_6)$ (mole%)	0.3	1.5	1.0	0.4
$S(C_2H_6)$ (%)	2.1	5.7	2.1	0.6
	MgO			
$X(CH_4)$ (%)	31.0	33.1	38.0	48.8
$Y(C_2H_6)$ (mole%)	1.8	1.7	1.4	0.9
$S(C_2H_6)$ (%)	5.8	5.1	3.7	1.8

Note. Column 1, pulse experiments with pure CH_4; columns 2–4, experiments with pulses of CH_4–O_2 mixtures with different CH_4–O_2 ratios.

Sequential Pulses of Oxygen and Methane

In these experiments a pulse sequence $O_2 \rightarrow CH_4 \rightarrow O_2 \rightarrow CH_4$ . . . with a constant interval between methane and oxygen pulses (see Methods) was applied. It should be mentioned that reaction products were observed only in the response to the methane pulse but not in the response to the oxygen pulse. This indicates that either oxidizable carbon-containing species on the surface (e.g., CH_xO) have only a very short lifetime or they do not stay on the surface at all.

(*a*) *Knudsen-Diffusion Regime*

Sm_2O_3. As described above, the yield of ethane passed through a maximum with increasing oxygen content in simultaneous pulses of CH_4 and O_2. The reaction of methane with adsorbed species was further investigated using experiments with sequential pulses of oxygen and methane: first the catalyst was treated by an oxygen pulse of high intensity to create a high concentration of adsorbed oxygen species on the surface; then after definite time intervals a methane pulse was introduced. The intensity of the oxygen pulse was 50 times higher than that of methane. During these experiments methane consumption started at 703 K; this temperature is equal to that at which oxygen started to interact with the catalyst surface (cf. Section I). At 1073 K, CH_4 was totally consumed when the interval between O_2 and CH_4 pulse was less or equal to 0.25 s, but no products were found. Most probably the methane is oxidized only to CO_2 which remained adsorbed on the catalyst. For time intervals of more than 2 s a significant increase in the CH_4 response, i.e., decreasing methane conversion, and an increasing CO response were detected while no C_2 hydrocarbons were observed.

(*b*) *Molecular-Diffusion Regime*

Sm_2O_3. The dependence of CH_4 conversion and product formation on the time interval between O_2 and CH_4 pulses (up to 5 s) at 1073 K is shown in Fig. 6. At short time intervals between oxygen and methane pulses (up to 0.25 s) a sharp increase in methane conversion accompanied by a decrease in C_2H_6 and CO formation was observed with decreasing time interval. Ethane formation first increased when increasing the time interval to 0.25 s, then it remained quite stable within 5 s (cf. Fig. 6), and even when methane was pulsed 20 s after oxygen the production of ethane was higher than during the reaction with lattice oxygen (Fig. 7).

Additional information can be derived from the temporal responses by comparing their shapes under different reaction conditions. The shapes of ethane and methane curves in the reaction of methane with lattice oxygen only differ from those in the presence of additional active

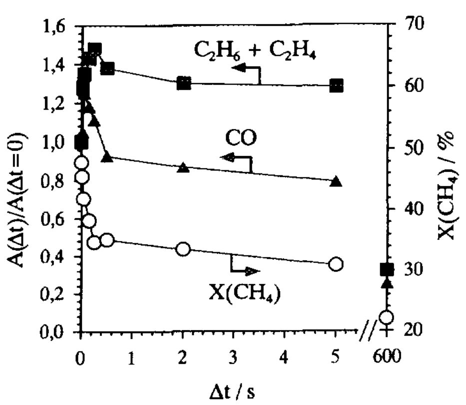

FIG. 6. Effect of the time interval (Δt) between the pulses of O_2 and CH_4 on the CH_4 conversion, and the product formation over Sm_2O_3 at 1073 K in the molecular-diffusion regime. The ordinate shows the ratio between the amounts formed at an offset time Δt to the respective amount for simultaneous pulsing (Δt = 0).

oxygen species formed by the interaction of gas-phase oxygen with the catalyst surface (Fig. 8). In the first case the ethane curve is broader than the methane response, as expected for product formation. In the second case, i.e., in the presence of adsorbed oxygen, the methane response is a little broader while the ethane curve shifts to shorter times and becomes even narrower than the methane response. This indicates that methyl radicals forming ethane are produced rapidly on the surface.

When pulsing CD_4 the same shifts of the C_2D_6 response curve to shorter time as for C_2H_6 curve in the reaction of CH_4 was observed while the curve of isotopic methane (CD_3H) became even broader in the presence of adsorbed oxygen (cf. Fig. 9).

MgO. The results of sequential pulsing of oxygen and methane in the molecular-diffusion regime are shown in Fig. 10. In contrast to Sm_2O_3 an increasing activity in methane consumption was observed only at time intervals up to 0.1 s. Increasing methane conversion accompanied only by increased CO_x formation was observed when the time interval between O_2 and CH_4 was decreased from 0.1 to 0 s.

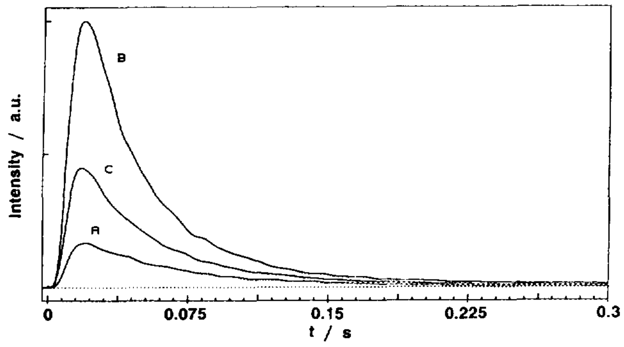

FIG. 7. Transient ethane formation during the reaction of methane over Sm_2O_3 in the molecular diffusion regime at 1073 K (A = pure CH_4 pulse over catalyst (10 min after oxidation)), B = simultaneous pulsing of CH_4 and O_2 (CH_4/O_2 = 1.5), C = sequential pulsing of O_2 and CH_4 with an interval of 20 s of the methane pulse.

When comparing the pulse shapes of methane and ethane in the reaction of methane with lattice oxygen and in the reaction of methane–oxygen mixtures over MgO it was found that, in the presence of oxygen, no shift of the ethane response to shorter times was observed.

DISCUSSION

The results described above will be discussed, and elementary processes occurring in the OCM reaction and in the H–D exchange in methane will be derived.

(*i*) *Heterogeneous Surface Processes in the OCM Reaction*

Adsorption. (1) Over Sm_2O_3 reversible adsorption of methane (Fig. 2) and ethane was observed under nonreactive conditions:

$$CH_4(g) \leftrightarrow CH_4(s) \quad T < 723 \text{ K } (\Delta H = -5 \pm 2 \text{ kJ/mol})$$
$$C_2H_6(g) \leftrightarrow C_2H_6(s) \quad T < 570 \text{ K } (\Delta H = -25 \pm 4 \text{ kJ/mol}).$$

(2) Strong adsorption of CO_2 occurs on the surfaces of both Sm_2O_3 and MgO possibly due to carbonate formation

$$CO_2(g) + O(sl) \leftrightarrow CO_3(s) \quad T < 1073 \text{ K},$$

where O(sl) denotes a surface lattice oxygen species.

(3) The reversible interaction of gas-phase O_2 with Sm_2O_3 is an activated process and takes place above 723 K (Fig. 4), presumably through dissociative adsorption

$$O_2(g) + 2\ {*} \leftrightarrow 2\ {*}O(s)$$

where * denotes a vacancy on the surface and *O(s) is an activated oxygen species without specified electronic charge.

(4) Over MgO no reversible interaction of CH_4 or O_2 with the catalyst surface was detected up to 1073 K.

Reaction. (1) The surface reaction of methane in the Knudsen regime in the absence of gas-phase O_2 results in the formation of methyl radicals and total oxidation products; no ethane or ethylene were, however, observed:

$$CH_4(g) + O(sl) \rightarrow CH_3\cdot(g) + OH(s).$$

These results confirm the findings of Lunsford and coworkers (8, 34) and Feng *et al.* (10), who also reported the direct detection of methyl radicals during the OCM reaction.

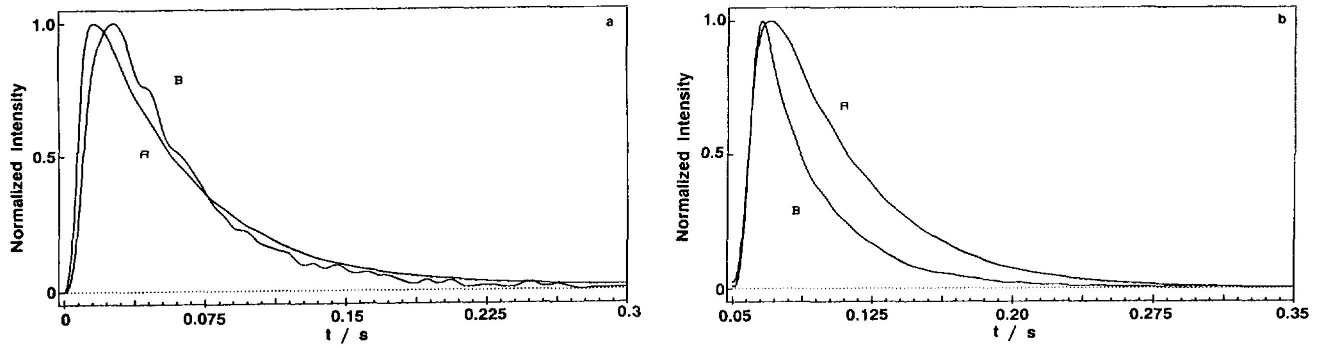

FIG. 8. Normalized transient responses for ethane formation over Sm_2O_3 during (a) the reaction of CH_4 over the catalyst surface (10 min after oxidation) (A = CH_4 (enhancement factor k = 1), B = C_2H_6 (k = 1321)) and (b) sequential pulses of O_2 and CH_4 with a time interval of 0.05 s (A = CH_4 (k = 1), B = C_2H_6 (k = 234)).

The yield of $CH_3\cdot$ passes through a maximum with increasing temperature accompanied by decreasing selectivity (Fig. 3). The increase in yield is certainly due to the higher surface activity at higher temperatures while the decrease may be explained by an increasing activity of the surface oxygen for the oxidation of radicals:

$$CH_3\cdot(g) + O(sl) \rightarrow CO_x.$$

However, the direct oxidation of methane to carbon oxides cannot be excluded:

$$CH_4(g) + O(sl) \rightarrow CO_x$$

$$CH_4(g) + {}^*O(s) \rightarrow CO_x.$$

For Sm_2O_3 the determined activation energy of 70 kJ/mol for the methane consumption is low compared to most of the reported values for the OCM reaction. It should be noted that at the low pressure inside the TAP reactor the probability of surface oxidation of methyl radicals compared to their gas-phase recombination is higher than in standard experiments at ambient pressures. Hence, the activation energy may correspond mainly to the reaction of direct oxidation of methyl radicals. It may also be ascribed to the much lower CO_2 coverage compared to experiments under steady-state at ambient pressure where the higher coverage may affect methane activation.

Results obtained from experiments in the molecular-diffusion regime demonstrated that ethane is formed in the gas phase by recombination of methyl radicals:

$$2CH_3\cdot(g) \rightarrow C_2H_6(g).$$

This confirms the widely accepted mechanism of ethane formation first proposed by Ito *et al.* (34). However, due to the high energy of free methyl radicals a third body molecule is most probably required in the gas phase to take away some of the excess energy of the ethane molecule after combination (methane itself may serve this purpose).

(2) The main product of the surface reaction of C_2H_6 with lattice oxygen of Sm_2O_3 was ethylene (Table 1):

$$C_2H_6(g) + 2O(sl) \rightarrow C_2H_4(g) + 2OH(s).$$

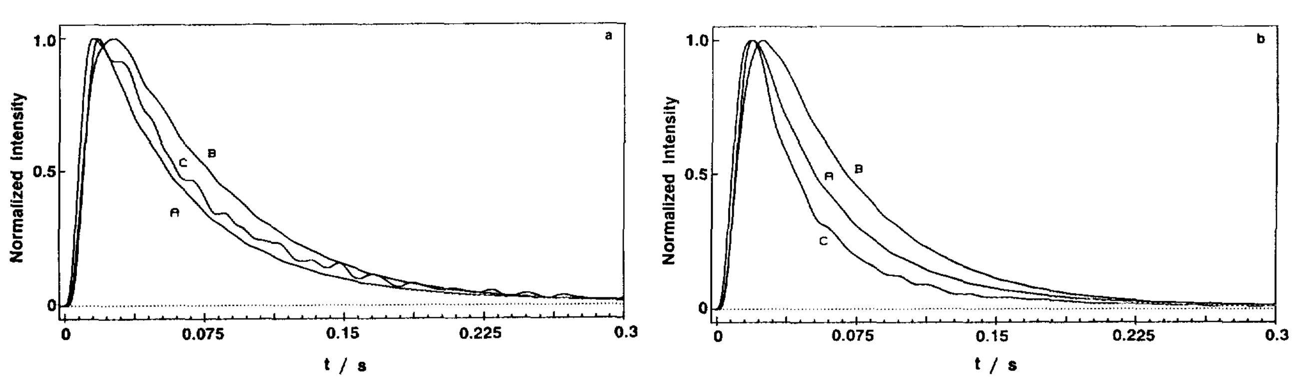

FIG. 9. Normalized transient responses for the formation of H–D exchange product (CD_3H) and ethane (C_2D_6) over Sm_2O_3 at 1073 K during (a) the reaction of CD_4 (A = CD_4 (enhancement factor k = 1), B = CD_3H (k = 38), C = C_2D_6 (k = 1142)) and (b) the reaction of CD_4/O_2 mixture of ratio 1/2 (A = CD_4 (k = 1), B = CD_3H (k = 12), C = C_2D_6 (k = 20)).

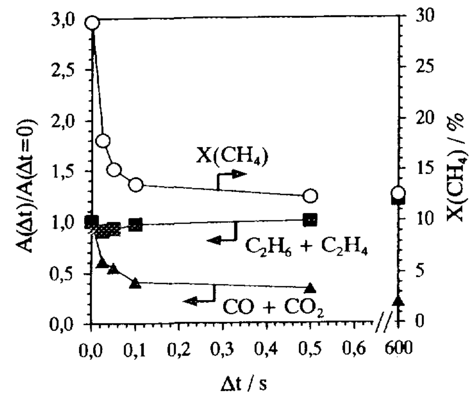

FIG. 10. Effect of the time interval (Δt) between the pulses of O_2 and CH_4 on the CH_4 conversion and the product formation over MgO at 1073 K in the molecular-diffusion regime. The ordinate shows the ratio between the amounts formed at an offset time Δt to the respective amount for simultaneous pulsing ($\Delta t = 0$).

Its selectivity decreased steadily with increasing temperature while the yield passed through a maximum at 991 K (Fig. 3). Also, ethane is converted to total oxidation products by surface lattice oxygen:

$$C_2H_6(g) + O(sl) \rightarrow CO_x.$$

The activity of the surface lattice oxygen for ethane conversion was much higher than for methane. For both molecules the total surface oxidation became significant with increasing temperature. Also Choudhary and Rane (15) reported that Sm_2O_3 catalyzes the conversion of ethane to ethylene in the absence of "free" gas-phase oxygen with a selectivity of 73% at 1073 K.

(3) It can be assumed that CO chemisorption or, more probably, its oxidation to CO_2 with formation of a strongly adsorbed species such as carbonate takes place on the surface of Sm_2O_3 in the absence of gas-phase oxygen:

$$CO(g) + O(sl) \rightarrow CO_2(s) \leftrightarrow CO_2(g).$$

Hereby, it was observed that the CO_2 responses at the reactor outlet are similar if either CO or CO_2 were pulsed at 1073 K. Hence, it can be assumed that CO_2 desorption from the surface is slow compared to the initial oxidation of CO; thus the rate-determining step under the applied conditions is the desorption and not the oxidation process. However, under steady-state conditions and therefore constant surface coverage of CO_2 the reaction of CO with oxygen might be rate limiting.

(*ii*) *The Role of Oxygen in the OCM Reaction*

A considerable difference in the properties of surface oxygen was found between MgO and Sm_2O_3 catalysts. Over **MgO** surface lattice oxygen species are responsible for methyl radical generation resulting in subsequent ethane formation as derived from experiments with single methane pulses and sequential pulsing of oxygen and methane. Additional adsorbed oxygen species have only very short lifetimes of less than 0.1 s and resulted in the formation of total oxidation products only (Fig. 10).

In contrast, $\mathbf{Sm_2O_3}$ activates gas-phase oxygen for selective methane conversion. Hence, $O_2(g)$ is not only necessary to replenish the surface after reaction of CH_4 but it also forms active species that exist on the surface for a rather long time (up to 20 s) before they desorb. These results are in agreement with the mechanism suggested by Amoerebieta and Colussi (35) for the OCM reaction at low pressures on Sm_2O_3. Statman *et al.* (25) also applied the TAP method to study the influence of the time difference between consecutive oxygen and methane pulses on the ethane formation over a Ba–Sr–Sm_2O_3 catalyst. They reported that even at a time interval of 30 s the activity was high. Hence, the surface residence times of oxygen species are in the same order of magnitude on both Sm_2O_3 and Ba–Sr–Sm_2O_3 catalysts.

The oxygen species (*O(s)) formed by interaction of gaseous O_2 with the catalyst surface are mainly responsible for methane activation and ethane formation over Sm_2O_3. Their activity towards the reaction of methane is higher compared to lattice oxygen; the lifetimes on the surface amounted up to 20 s (cf. Fig. 6 and 7). It was assumed that these species accelerate the conversion of methane to methyl radicals (cf. Fig. 8) which then combine to ethane in the gas phase. The present results of the simultaneous pulsing of CH_4–O_2 (cf. Table 3) indicate that the concentration of oxygen sites on the surface mainly determines the product selectivity: a high concentration favours total oxidation while lower concentrations result in the formation of selective products. From the results of sequential pulsing of O_2 and CH_4 (cf. Fig. 6 for Sm_2O_3 and Fig. 10 for MgO) it may be suggested that at short time intervals methane is converted mainly to CO_2 due to reaction with weakly adsorbed oxygen, i.e., oxygen species with relatively short lifetimes. Another reason for this high activity might be the high concentration of active oxygen species on the catalyst surface at short time intervals between the pulses as mentioned above.

In spite of the much lower reactivity compared to adsorbed oxygen lattice oxygen can also convert methane to ethane and CO_x. This is in contrast to results published by Ekstrom and Lapszewicz (36), Kalenik and Wolf (27), and Choudhary and Rane (15), who have reported that the activity of lattice oxygen of Sm_2O_3 for the conversion of methane is approximately zero. However, it can be assumed that due to the very small amount of methane pulsed over the surface in the TAP experiments compared to conventional pulse or isotopic switching experiments the reactivity of the lattice oxygen had been detected more accurately in the present work.

(iii) Methane Activation in H–D Exchange and OCM Reaction

D–H exchange. Over both catalysts D–H exchange of CD_4–CH_4 mixtures and pure CD_4 with the surface was observed. The product distribution and the CD_4 conversion were similar in both experiments; hence, it can be concluded that under the reaction conditions applied no direct interaction between methane molecules on the surface proceeds. All methane molecules exchange only with hydrogen present on the surface, most probably with hydroxyl groups as described by Larson and Hall (37) for alumina and silica–alumina. Due to the high mobility of surface hydrogen at elevated temperature all hydrogen can take part in this reaction. This is further supported by the results of the CD_4 multipulsing experiment; the decreasing amount of exchange products observed with increasing number of CD_4 pulses can be explained by the replacement of OH-groups by OD-groups on the surface. The longer residence times of the exchanged methanes compared to CD_4 indicates that a rather strong interaction of methane with the surface takes place. It might be assumed that heterolytic dissociation of methane on the surface is involved in the H–D exchange reaction as proposed by Utajama *et al.* (20):

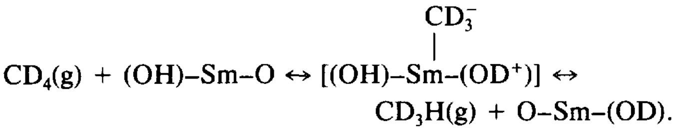

$$CD_4(g) + (OH)\text{–}Sm\text{–}O \leftrightarrow [(OH)\text{–}\overset{\overset{CD_3^-}{|}}{Sm}\text{–}(OD^+)] \leftrightarrow CD_3H(g) + O\text{–}Sm\text{–}(OD).$$

To elucidate the mechanism and to distinguish between single- or multiple-step H–D exchange the isotopic distribution of the products was analyzed. From the distribution and especially from the pulse shapes of the isotopic methanes it is obvious that for all temperatures the exchange was controlled by kinetics and was not in an equilibrium state. Hence, the isotopic distribution should correspond to a binomial distribution if the exchange reaction proceeds exclusively with a single-step D–H exchange. The calculation of the distribution was complicated because of the formation of methyl radicals and CO_x simultaneously with the exchange reaction. On the oxidized surfaces the product distributions did not correspond to the binomial distribution possibly due to different degrees of oxidation of the different isotopic methanes to CO_x. CD_4 and the exchanged methanes which are formed first, e.g., CD_3H, have a higher probability to be oxidized than the products that are formed later, e.g., CDH_3. However, the simple stepwise mechanism cannot be confirmed and hence it is not possible to exclude the involvement of multiple exchange over the oxidized surfaces of MgO and Sm_2O_3. Also Shestakov *et al.* (38) postulated that the H–D exchange over Sm_2O_3(1%)/MgO has both single- and multiple-step character.

When CD_4 was pulsed over a H_2-prereduced catalyst surface the product distribution fits a binomial distribution, confirming a stepwise mechanism with one H–D transfer per step under these conditions.

OCM reaction. It is widely accepted that in methane activation for the coupling reaction the abstraction of a H atom by the catalyst surface is the first step resulting in the formation of a methyl radical which is then immediately released into the gas phase (8).

On $\mathbf{Sm_2O_3}$ the main activity for methyl-radical formation is provided by strongly adsorbed oxygen species formed on the surface during its interaction with gas-phase O_2. From the TAP results it can be concluded that the presence of adsorbed oxygen species strongly accelerates the formation of methyl radicals which then combine to ethane. However, the exchange reaction, i.e., the formation of CD_3H, was not influenced (cf. Fig. 9). Hence, it can be assumed that the type of methane activation which takes place in the H–D exchange is not involved in the OCM reaction over Sm_2O_3. In this context, it is not surprising that no correlation was found between the rate of H–D exchange and methane conversion as reported by Lapszewicz and Jiang (16) for Sm_2O_3, MgO, and γ-Al_2O_3 catalysts.

In contrast to results of Ekstrom and Lapszewicz (36) who reported that a pool of adsorbed CH_4 exists under reaction conditions on Sm_2O_3 and of Amorebieta and Colussi (35) who proposed a competitive adsorption of methane and oxygen on the same sites, in the present work no reversible adsorption of methane could be detected under reaction conditions on both catalysts (MgO and Sm_2O_3) based on the moment analysis of the response signal.

Due to the fast formation of ethane in the presence of surface oxygen species formed by the interaction of gaseous O_2 it can be assumed that methyl radicals are formed by direct interaction of gas-phase CH_4 with these oxygen species in an Eley–Rideal type of mechanism. The same mechanism was proposed by several authors in the past (8–11, 35).

Over **MgO** the presence of gas-phase O_2 resulting in adsorbed oxygen on the surface (experiments with sequential pulsing oxygen and methane) had no beneficial effect on the ethane formation: compared to the reaction of a single methane pulse with lattice oxygen a smaller amount of ethane was produced and no acceleration of the ethane formation was observed when gas-phase O_2 was present. It might be therefore assumed that the activation of methane towards methyl radical formation in the OCM reaction proceeds only by participation of lattice oxygen species, possibly via dissociative adsorption as assumed in Ref. (20) for this catalyst. This is supported by the observation that in contrast to the above-mentioned results for Sm_2O_3 the dynamics of the ethane formation which is represented by its response curve was not influenced by the presence of gas-phase O_2 and/or adsorbed oxygen species.

CONCLUSIONS

A transient technique with high time resolution was used to elucidate heterogeneous reaction steps in the OCM reaction over Sm_2O_3 and MgO. The results showed that lattice oxygen species are active for the conversion of methane to methyl radicals, the dehydrogenation of ethane to ethylene, and the oxidation of methane, ethane, and CO. However, the activity of the catalysts is much higher if additional oxygen species (*O(s)) which have been formed on the surface by the interaction with gas-phase oxygen are present. The properties of these species depend strongly on the catalyst; on MgO they only catalyze the formation of total oxidation products while on Sm_2O_3 the most important step of the OCM reaction, i.e., the formation of methyl radicals combining to ethane, is accelerated and enhanced by these species. The methane activation during the H-D exchange proceeds with participation of surface hydrogen possibly via dissociative adsorption; this process is most probably not directly involved in the formation of methyl radicals over Sm_2O_3. Based on the presented results it is not possible to clarify the type of the active oxygen species (e.g., O_2^-, O_2^{2-}, O^-) and their surface concentration. For this purpose, further experiments concerning the role of oxygen in the OCM reaction have to be carried out.

ACKNOWLEDGMENTS

This work was partly supported by the European Community (Contract JOUF 0044). The support of Deutsche Forschungsgemeinschaft for a postdoctoral fellowship (to O.V.B.) is also acknowledged.

REFERENCES

1. Cant, N. W., Lukey, C. A., Nelson, P. N., and Tyler, R. J., *J. Chem. Soc., Chem. Commun.*, 766 (1988).
2. Buyevskaya, O. V., Suleimanov, A. I., Aliev, S. M., and Sokolovskii, V. D., *React. Kinet. Catal. Lett.* **33,** 223 (1987).
3. Nelson, P. F., Lukey, C. A., and Cant, N. W., *J. Catal.* **120,** 216 (1989).
4. Otsuka, K., Inaida, M., Wada, Y., Komatsu, T., and Morikawa, A., *Chem. Lett.* 1531 (1989).
5. Mirodatos, C., Holmen, A., Mariscal, R., and Martin, G. A., *Catal. Today* **6,** 601 (1990).
6. Burch, R., Tsang, S. C., Mirodatos, C., and Sanchez, J. G., *Catal. Lett.* **7,** 423 (1990).
7. Lehmann, L., and Baerns, M., *Catal. Today* **13,** 265 (1992).
8. Driscoll, D. J., Martir, W., Wang, J.-X., and Lunsford, J. H., *J. Am. Chem. Soc.* **107,** 58 (1985).
9. Dubois, J.-L., and Cameron, C. J., *Appl. Catal.* **67,** 49 (1990).
10. Feng, Y., Niiranen, J., and Gutman, D., *J. Phys. Chem.* **95,** 6558 (1991).
11. Tung, W.-Y., and Lobban, L. L., *Ind. Eng. Chem. Res.* **31,** 1621 (1992).
12. Bytyn, W., and Baerns, M., *Appl. Catal.* **28,** 199 (1986).
13. Sokolovskii, V. D., Aliev, S. M., Buyevskaya, O. V., and Davydov, A. A., *Catal. Today* **4,** 293 (1989).
14. Hatano, M., and Otsuka, K., *J. Chem. Soc., Faraday Trans. 1* **85,** 199 (1989).
15. Choudhary, V. R., and Rane, V. H., *J. Catal.* **130,** 411 (1991).
16. Lapszewicz, J., and Jiang, X., *Catal. Lett.* **13,** 103 (1992).
17. Robertson, P. J., Scurrell, M. S., and Kemball, C., *J. Chem. Soc., Faraday Trans. 1* **71,** 903 (1975).
18. Robertson, P. J., Scurrell, M. S., and Kemball, C., *J. Chem. Res. Synop.*, 36 (1977).
19. Bird, R., Kemball, C. and Leach, H. F., *J. Catal.* **107,** 424 (1987).
20. Utajama, M., Hattori, H., and Tanabe, K., *J. Catal.* **53,** 237 (1978).
21. Asami, K., Shikada, T., Fujimoto, K., and Tominaga, H., *Ind. Eng. Chem. Res.* **26,** 2348 (1986).
22. Hatano, M., and Otsuka, K., *Inorg. Chim. Acta* **146,** 243 (1988).
23. Otsuka, K., and Said, A. A., *Inorg. Chim. Acta* **132,** 123 (1987).
24. Peil, K. P., Goodwin, J. G. and Marcelin, G., *J. Catal.* **131,** 143 (1990).
25. Statman, D. J., Gleaves, J. T., McNamara, D., Mills, P. L., Fornasari, G., and Ross, J. R. H., *Appl. Catal.* **77,** 45 (1991).
26. Kalenik, Z., and Wolf, E. E., *Catal. Lett.* **11,** 309 (1991).
27. Kalenik, Z., and Wolf, E. E., *Catal. Lett.* **9,** 441 (1991).
28. Lisachenko, A. A. and Filimonov, V. N., *Dokl. Akad. Nauk SSSR* **177,** 391 (1967).
29. Eick, H. A., Baenziger, N. C., and Eyring, L., *J. Am. Chem. Soc.* **78,** 5987 (1956).
30. Gleaves, J. T., Ebner, J. R., and Kuechler, T. C., *Catal. Rev.—Sci. Eng.* **30,** 49 (1988).
31. Dibeler, V. H., and Mohler, F. L., *Res. Nat. Bureau Stand.* **45,** 2155 (1950).
32. Gulcicek, E. E., Colson S. D., and Pfefferle, L. D., *J. Phys. Chem.* **94,** 7069 (1990).
33. Lee, S.-P., Yu, T., and Lin, M. C., *Int. J. Chem. Kinet.* **22,** 975 (1990).
34. Ito, T., Wang, J.-X., Lin, C.-H., and Lunsford, J. H., *J. Am. Chem. Soc.* **107,** 5062 (1985).
35. Amorebieta, V. T., and Colussi, A. J., *J. Phys. Chem.* **93,** 5155 (1989).
36. Ekstrom, A., and Lapszewicz, J. A., *J. Am. Chem. Soc.* **110,** 5226 (1988); Ekstrom, A., and Lapszewicz, J. A., *J. Phys. Chem.* **93,** 5230 (1989).
37. Larson, J. G., and Hall, W. K., *J. Phys. Chem.* **69,** 3080 (1965).
38. Shestakov, A. F., Tyulenin, Yu, P., Kadushin, A. A., Seleznev, V. A., and Platé, S. E., *Kinet. Catal.* (*Engl. Transl.*) **33,** 462 (1992).